Global Change Biology

Global Change Biology (2012) **18**, 493–503, doi: 10.1111/j.1365-2486.2011.02575.x

Nitrogen source and pCO_2 synergistically affect carbon allocation, growth and morphology of the coccolithophore *Emiliania huxleyi*: potential implications of ocean acidification for the carbon cycle

STEPHANE C. LEFEBVRE, INA BENNER, JONATHON H. STILLMAN, ALEXANDER E. PARKER, MICHELLE K. DRAKE, PASCALE E. ROSSIGNOL, KRISTINE M. OKIMURA, TOMOKO KOMADA and EDWARD J. CARPENTER

Romberg Tiburon Center, San Francisco State University, Tiburon, CA 94920, USA

Abstract

Coccolithophores are unicellular phytoplankton that produce calcium carbonate coccoliths as an exoskeleton. *Emiliania huxleyi*, the most abundant coccolithophore in the world's ocean, plays a major role in the global carbon cycle by regulating the exchange of CO_2 across the ocean-atmosphere interface through photosynthesis and calcium carbonate precipitation. As CO_2 concentration is rising in the atmosphere, the ocean is acidifying and ammonium (NH_4^+) concentration of future ocean water is expected to rise. The latter is attributed to increasing anthropogenic nitrogen (N) deposition, increasing rates of cyanobacterial N_2 fixation due to warmer and more stratified oceans, and decreased rates of nitrification due to ocean acidification. Thus, future global climate change will cause oceanic phytoplankton to experience changes in multiple environmental parameters including CO_2, pH, temperature and nitrogen source. This study reports on the combined effect of elevated pCO_2 and increased NH_4^+ to nitrate (NO_3^-) ratio (NH_4^+/NO_3^-) on *E. huxleyi*, maintained in continuous cultures for more than 200 generations under two pCO_2 levels and two different N sources. Herein, we show that NH_4^+ assimilation under N-replete conditions depresses calcification at both low and high pCO_2, alters coccolith morphology, and increases primary production. We observed that N source and pCO_2 synergistically drive growth rates, cell size, and the ratio of inorganic to organic carbon. These responses to N source suggest that, compared to increasing CO_2 alone, a greater disruption of the organic carbon pump could be expected in response to the combined effect of increased NH_4^+/NO_3^- ratio and CO_2 level in the future acidified ocean. Additional experiments conducted under lower nutrient conditions are needed prior to extrapolating our findings to the global oceans. Nonetheless, our results emphasize the need to assess combined effects of multiple environmental parameters on phytoplankton biology to develop accurate predictions of phytoplankton responses to ocean acidification.

Keywords: calcification, carbon, global climate change, nitrogen, ocean acidification, phytoplankton

Received 30 August 2011; revised version received 30 August 2011 and accepted 1 September 2011

Introduction

The coccolithophore *Emiliania huxleyi* (Lohmann) Hay and Mohler originated approximately 270 000 years ago (Thierstein *et al*., 1977), and despite its relatively young existence has colonized almost every photic zone of the modern world ocean, making it one of the most abundant, successful and ubiquitous species of marine phytoplankton. *E. huxleyi* is a unicellular phytoplankton species that produces intricate calcium carbonate platelets (coccoliths) as an exoskeleton, and in summer forms extensive blooms spanning wide oceanic areas at high latitudes. Most of the organic carbon deposition in the deep sea has been shown to be carried by calcium carbonate (Armstrong *et al*., 2002; Francois *et al*., 2002) and coccolithophore calcium carbonate ballast has been estimated to account for up to 83% of the organic carbon flux to the seafloor (Zondervan *et al*., 2001; Klaas & Archer, 2002). These features have contributed to the establishment of *E. huxleyi* as a major contributor to the global carbon cycle by regulating the exchange of CO_2 across the ocean–atmosphere interface through photosynthesis and calcium carbonate precipitation (de Vargas *et al*., 2007), and export of carbon to the deep ocean (Zondervan *et al*., 2001; Klaas & Archer, 2002).

Present and future anthropogenic emissions of CO_2 to the atmosphere are predicted to change physicochemical properties of the oceans. In addition, to increases in temperature and enhanced stratification

Correspondence: Stephane C. Lefebvre, tel. + 1 415 338 3788, fax + 1 415 435 7120, e-mail: stephane@rtc.sfsu.edu

brought about by climate change, increased partial pressure of CO_2 (pCO_2) in surface waters decreases pH and carbonate ion concentration ($[CO_3^{2-}]$), a phenomenon termed ocean acidification (Samiento *et al*., 1998; Rost & Riebesell, 2004).

Recent studies indicate that the N cycle may respond strongly to changes in atmospheric pCO_2, and that increasing pCO_2 may increase the NH_4^+/NO_3^- ratio in surface waters (Hutchins *et al*., 2009; Wyatt *et al*., 2010; Beman *et al*., 2011). Four independent studies (Barcelos e Ramos *et al*., 2007; Hutchins *et al*., 2007; Levitan *et al*., 2007; Kranz *et al*., 2009) suggest that nitrogen gas (N_2) fixation rates by *Trichodesmium* will increase by 35–65% by the end of the century due to increased atmospheric pCO_2. The nitrifying bacterium *Nitrosococcus oceanus* has optimal growth at pH 8, but is inhibited at lower pH (Ward, 1987). Microbial nitrification rates were shown to decrease when pH was experimentally reduced at multiple locations in the Atlantic and Pacific Oceans (Huesemann *et al*., 2002; Beman *et al*., 2011).

In ocean surface waters, inorganic N is encountered predominantly as NO_3^-, nitrite (NO_2^-) and NH_4^+ ions and is often considered one of the major limiting elements that restrict marine eukaryotic phytoplankton cellular and metabolic processes (Dugdale, 1967; Ryther & Dunstan, 1971). Surface-water NO_3^- concentrations range widely, from the analytical detection limit (3–15 nM) (Holmes *et al*., 1999) to about 50 μM, as a function of both space (e.g., proximity to land and river mouths) and time (e.g., upwelling events; phytoplankton community blooms and terminations). In contrast, NH_4^+ concentrations vary from below the detection limit in most open ocean waters to about 2 μM in coastal waters and estuaries (Sharp, 1983; Sharp *et al*., 2009). Although NO_3^- can be found at very high concentrations in surface water in upwelling areas, in oligotrophic waters NH_4^+ is often the dominant N source used by phytoplankton. In oligotrophic waters, NO_3^- is supplied slowly to the euphotic zone while NH_4^+ is recycled *in situ*. NH_4^+ is also taken up as fast as it is produced, thereby, explaining the very low concentration generally found in the open ocean. In addition, NH_4^+ requires less reducing power for cellular assimilation relative to NO_3^- assimilation, making this source of N less costly to metabolize (Mulholland & Lomas, 2008).

The primary effects of ocean acidification on marine organisms have been subject to intense research for the past decade (Kroeker *et al*., 2010). However, studies of phytoplankton that focus on secondary effects of ocean acidification, whereby acidification directly impacts other environmental parameters and thus indirectly impacts phytoplankton biology are rare and have only recently been reported (Shi *et al*., 2010). In future ocean water, phytoplankton species will experience change in CO_2 and will also respond to concomitant change of other environmental parameters brought about by global climate change. In this report, we have investigated the combined effect of predicted increased pCO_2 and increased NH_4^+/NO_3^- ratio in a calcifying coccolithophore *E. huxleyi*, revealing for the first time that N source and pCO_2 synergistically drive growth rates, cell size, and the ratio of inorganic to organic carbon.

Materials and methods

Phytoplankton species and culturing

Monospecific nutrient-replete cyclostat cultures of *E. huxleyi* (calcifying strain CCMP 371) from the Provasoli-Guillard CCMP (East Boothbay, ME, USA) were grown at 17 °C, using 0.2 μm filtered nutrient-poor aged seawater (Half Moon Bay water, 37° 29′ 31″ N, 122° 30′ 02″ W, collected October 18th and 24th 2008) with metals and vitamins added to achieve f/2 trace element concentrations (Guillard & Ryther, 1962). Phosphate was supplied as 14 μM of NaH_2PO_4 and N was supplied as either a mixture of 100 μM NH_4Cl + 100 μM $NaNO_3$ (hereafter referred to as $NH_4^+ + NO_3^-$ treatment) or as 200 μM $NaNO_3$ (hereafter referred to as NO_3^- treatment). The pCO_2 levels in the cultures were controlled by aeration with gas mixtures of pure CO_2 and air (scrubbed free of NH_4^+ by passage through a diluted phosphoric acid trap) to achieve CO_2 levels of 400 and 1000 ppm. The pCO_2 input to the culture was continuously monitored using an infra-red gas analyzer (LI-820, LI-COR, Lincoln, NE, USA). One *E. huxleyi* cyclostat culture for each condition was maintained under continuous flow in cylindrical 10 L borosilicate glass culture vessels. Despite great care to avoid bacterial contamination of the cultures, bacteria-free cultures could not be maintained during the length of the experiment. Nevertheless, the abundance of free and attached bacteria, counted at the beginning, in the middle and at the end of the sampling program by DAPI direct counts, were similar across the four treatments and remained stable and proportional to the cell abundance of *E. huxleyi* ($<5 \times 10^9$ cell L^{-1}), suggesting that bacterial carbon and activity were negligible compared to those of *E. huxleyi*. A cell density of 500 cells μL^{-1} (around 25% of the maximum yield under high-light conditions for the inflow nutrient levels) was the target density and the inflow medium flow rate was adjusted daily to maintain steady cell abundance. Cultures were continuously agitated by gentle stirring to ensure homogenous cell suspension and avoid possible light and nutrient gradient effects. Cultures were illuminated on a light/dark cycle of 16/8 h with cool-white fluorescent lamps (Vita-Lite 5500K, DUROTEST, Philadelphia, PA, USA) at photon flux densities (PFDs) of 450–500 μmol photons m^{-2} s^{-1} to mimic the light regime and light intensity during summer at high latitude. PFD was measured in the center of each vessel containing *E. huxleyi* culture using a 4π Biospherical instruments (San Diego, CA, USA) probe, model QSP170B. This high-light level has previously been shown to ensure at least 50% of maximal photosynthetic activity without causing

photoinhibition in *E. huxleyi* (Nanninga & Tyrrell, 1996; Feng *et al*., 2008).

Sampling

Cultures were maintained under each condition for 214 to 291 generations (over 5 months of continuous culturing) before sampling every other day over a 2 to 3 weeks period, with steady-state re-established between each sampling date. The intense amount of labor required to maintain cyclostats of this kind prevented us from running each treatment in duplicate or triplicate as is commonly done for bottle experiments. Instead, since our growth rates were higher than 0.7 day^{-1} (more than one division per day, Table 1), by sampling every third day we ensured that the population of cells had been replaced completely between collection days. Therefore, this sampling strategy allowed for repeated sampling of the culture vessels to be taken and is routinely used for continuous culture (Sciandra *et al*., 2003; Leonardos & Geider, 2005; Lefebvre *et al*., 2010). Samples for calcification rate measurements were taken when the cultures were at steady state (cell density variation was 10% or less for three consecutive days), at 4 and 12 h into the light phase and 4 h into the dark phase. Samples for total particulate carbon (TPC), particulate organic carbon and nitrogen (POC, PON), dissolved inorganic carbon (DIC), scanning electron microscopy (SEM), were collected 14 h after the light onset. In addition, at each sampling, aliquots of each culture were taken for routine cell count, cell size, and determination of total alkalinity and nutrients.

Aqueous chemistry

Samples for nutrient analysis were collected by filtration through a 0.2 μm polycarbonate filter in 50 mL polycarbonate tubes rinsed twice with double distilled water and stored at −20 °C until analysis. Nutrient concentrations were determined within 2 weeks of collection. The $NO_3^- + NO_2^-$ and phosphate concentrations were measured according to Whitledge *et al.* (1981), using a Bran and Luebbe Autoanalyser II (Bran Luebbe, Inc. Buffalo Grove, IL, USA). The NH_4^+ levels were determined according to Solorzano (1969), using a HP Diode Array spectrophotometer model 8452A.

Total alkalinity (TA) was measured by potentiometric titration (Bradshaw *et al*., 1981) using a Metrohm Dosimat 765 (Metrohm, Herisau, Switzerland) and a high sensitivity combined electrode (Fisher # 13-642-237) and the end point determined from linear Gran plots (Gran, 1952). Changes of pH in the cultures were measured using the same instrument as above. The pH electrode was calibrated daily with standard NBS buffer solution (Fisher # SB105) and measured pH values were later converted to SW scale using the program CO2SYS (Lewis & Wallace, 1998). Salinity was determined just before TA measurements using a YSI salinometer (YSI Incorporated, Yellow Springs, OH, USA). For TA and pH measurements, seawater was equilibrated at 25 °C and water temperature was recorded continuously during the measurements to minimize inaccuracy associated with temperature fluctuation. Dissolved inorganic carbon (DIC) was measured according to Friederich *et al.* (2002) except that the N_2 carrier gas was replaced by pure O_2. The TA and DIC values were standardized against a Dickson standard (batch #96, Marine Physical Laboratory, Scripps Institution of Oceanography, La Jolla, CA, USA). Concentrations of the carbonate species were calculated from temperature, salinity, DIC, TA, PO_4^{2-}, and silicate concentrations using the program CO2SYS (Lewis & Wallace, 1998), and using the equilibrium constants of Mehrbach *et al.* (1973) refitted by Dickson & Millero (1987).

Physiologic and elemental analyses of the cultures

Culture cell size was determined by flow cytometry with a Cytobuoy type CYTOSIFT (Cytobuoy.Co, Woerden, the Netherlands). Samples for determination of TPC and POC were filtered on pre-combusted (4 h, 450 °C) GF/F-filters (Whatman, approximately 0.7 μm) and dried at 55 °C. Prior to analysis, the POC filters were washed with 230 μL of 1 N HCl to remove inorganic carbon. The TPC and POC were measured on a Costech ECS 4010 CHNSO analyzer (Costech Analytical Technologies Inc., Valencia, CA, USA). Particulate inorganic carbon (PIC) was calculated as the difference between TPC and POC.

Table 1 Parameters of the seawater carbonate system in *Emiliania huxleyi* cultures

Treatment	LCO_2 $NH_4^+ + NO_3^-$	LCO_2 NO_3^-	HCO_2 $NH_4^+ + NO_3^-$	HCO_2 NO_3^-
DIC (μmol $kgSW^{-1}$)	1862 (a) ± 14	1837 (a) ± 15	2112 (b) ± 8	1980 (c) ± 16
HCO_3^- (μmol $kgSW^{-1}$)	1577 (a) ± 38	1574 (a) ± 7	1914 (b) ± 11	1769 (c) ± 23
CO_3^{2-} (μmol $kgSW^{-1}$)	285 (a) ± 20	231 (b) ± 8	186 (b) ± 6	190 (b) ± 8
pCO_2 (μmol $kgSW^{-1}$)	5.9 (a) ± 0.7	6.9 (a) ± 0.3	13 (b) ± 0.6	11 (b) ± 0.8
pCO_2 (ppm)	166 (a) ± 20	194 (a) ± 7	367 (b) ± 16	308 (b) ± 23
TA (μmol $kgSW^{-1}$)	2278 (a) ± 18	2190 (b) ± 16	2379 (c) ± 11	2258 (a,b) ± 11
pH (SW scale)	8.35 (a) ± 0.04	8.28 (a) ± 0.01	8.08 (b) ± 0.02	8.13 (b) ± 0.02
Ω calcite	6.8 (a) ± 0.5	5.7 (b) ± 0.2	4.5 (c) ± 0.2	4.6 (c) ± 0.2

Data are shown for the four cultures in each growing conditions. Low CO_2 (LCO_2) and high CO_2 (HCO_2) with $NH_4^+ + NO_3^-$ or NO_3^- as N source. Samples were taken 14 h into the light period. Data are given as means ± SE for at least four replicates taken every third day for each culture condition. Letters in parentheses indicate significant differences ($P < 0.01$) among treatment types using analysis of variance (ANOVA), Tukey's *post hoc* test. DIC, dissolved inorganic carbon; HCO_3^-, bicarbonate; CO_3^{2-}, carbonate; pCO_2, partial pressure of CO_2 in seawater; TA, total alkalinity; Ω, calcite saturation state.

Calcification rates were determined using ^{14}C according to Balch *et al.* (1992). Briefly, 30.6 μCi $H^{14}CO_3$ was added to 50 mL of culture aliquoted in transparent flasks. All replicates were incubated for 30 min under the growing condition before stopping the reaction by addition of 0.1% mercuric chloride. Controls were spiked with 0.1% mercuric chloride before incubation. Samples were collected onto pre-combusted GF/F-filters, half of which were placed in scintillation vials with 6.5 mL Optiphase 'Hisafe' 3 scintillation cocktail (PerkinElmer, Inc., San Jose, CA, USA). The other half were treated with 250 μL of 1 N HCl to remove inorganic carbon prior being placed in scintillation vials. Scintillation cocktail was added after 24 h. The ^{14}C incorporation was measured with a 1414 Liquid Scintillation Counter (PerkinElmer, Inc.). Calcification rate was calculated with the difference of the nonacidified and acidified filter radioactivity. Calcification rates and primary production rates in the middle of the dark phase were negligible (0.02 pg C $cell^{-1}$ h^{-1} ± 0.01 SE and 0.0050 pg C $cell^{-1}$ h^{-1} ± 0.0005 SE, respectively) and have not been represented on the figures.

The NO_3^- and NH_4^+ uptake rates were measured using ^{15}N tracer techniques. From each culture, replicate 25 mL samples were aliquoted into clear 50 mL culture flasks. Additions of either $^{15}NH_4Cl$ or $K^{15}NO_3$ (99 at.% ^{15}N, Cambridge Isotope Laboratories, Inc., Andover, MA, USA) were made to achieve an isotopic enrichment of 20 at.% ^{15}N. In the NO_3^--only treatment, 5 μmol L^{-1} $^{15}NH_4^+$ was added resulting in isotopic enrichment >95 at.% $^{15}NH_4^+$. Incubations were performed over 1 h under culture growth conditions and were terminated by gentle vacuum filtration onto pre-combusted (450 °C for 4 h) 25 mm diameter GF/F filters. The PON and ^{15}N enrichment were determined using a PDZ Europa 20/20 gas chromatograph – mass spectrometer. The N transport (ρ, μmol L^{-1} day^{-1}) was calculated according to Dugdale & Wilkerson (1986) and normalized to cell abundance.

Samples for SEM imaging were prepared by filtering 3 mL of culture on 0.2 μm pore size polycarbonate filters (Millipore, Billerica, MA, USA). Filters were dried at 60 °C for 16 h. Thereafter, pieces of the filters were sputter-coated with gold–palladium and imaged with a ZEISS Ultra 55 Field Emission SEM (Carl Zeiss Microscopy, LLC, Peaboy, MA, USA).

Statistical analysis

All statistical analyses were performed using analysis of variance (ANOVA) in R v.2.6.2 (http://www.r-project.org). Significant differences in parameters across treatments (at a given *P* value), are reported on graphics and tables as different letters unless indicated otherwise. Same letter indicates nonsignificant difference at the given *P* value.

Results

To analyze the effect of pCO_2 levels and N sources on the physiology of *E. huxleyi* we grew cells under four different culture conditions: low pCO_2 and a mix of $NH_4^+ + NO_3^-$ (LCO_2 $NH_4^+ + NO_3^-$), low pCO_2 and NO_3^- as sole source of N (LCO_2 NO_3^-), high pCO_2 and $NH_4^+ + NO_3^-$ (HCO_2 $NH_4^+ + NO_3^-$) and high pCO_2 and NO_3^- (HCO_2 NO_3^-). First we monitored the water chemistry parameters in the cultures. pH and pCO_2 exhibited dynamic diurnal variations, with pCO_2 values increasing at night and decreasing during the light phase, while pH followed the opposite pattern (Fig. S1). pCO_2 levels in the culture vessels were lower than our aimed targets, averaging 240 ± 30 ppm and 580 ± 40 ppm (mean ± SE) in the middle of the dark phase for the cultures bubbled with 400 and 1000 ppm CO_2, respectively. These values decreased to 190 ± 10 ppm and 340 ± 20 ppm (mean ± SE) toward the end of the light phase indicating that the cultures were actively depleting CO_2 through photosynthesis. Regardless of N treatment, HCO_2 reduced pH by 0.21 units on average compared to LCO_2 (Table 1). pH was not affected by the presence of NH_4^+. Under LCO_2, DIC, bicarbonate ion concentration [HCO_3^-], and pCO_2 were similar between $NH_4^+ + NO_3^-$ and NO_3^- cultures, but [CO_3^{2-}], TA, and calcite saturation state (Ω calcite) were higher in the $NH_4^+ + NO_3^-$ culture (Table 1). Under HCO_2, pCO_2, [HCO_3^-] and DIC were higher relative to LCO_2 for both N treatments, but this offset was greater in the $NH_4^+ + NO_3^-$ culture (Table 1). At the same time, [CO_3^{2-}] and Ω calcite were lower under HCO_2 relative to LCO_2, and again, this offset was greater for the $NH_4^+ + NO_3^-$ culture (Table 1). For both $NH_4^+ + NO_3^-$ and NO_3^- cultures, TA was higher under HCO_2 relative to LCO_2 by an average of 4%.

Total N concentration was provided at 200 μM in the cultures to obtain sufficient biomass and to insure that N was not limiting. In $NH_4^+ + NO_3^-$, NH_4^+ concentration used was 100 μM. To test the potential toxic effect of NH_4^+, we assessed the NH_4^+ toxicity threshold for our strain of *E. huxleyi* by measuring growth rates and maximum PSII efficiency through a range of NH_4^+ concentrations. *E. huxleyi* growth rates and maximum PSII efficiency were not affected along the range 50–500 μM (Fig. S2, Table S1). The NH_4^+ was shown to become toxic to *E. huxleyi* at concentrations of 1 mM and above. During *E. huxleyi* culturing for 214 to 291 generations (Table 2), excess nutrients always remained in the media. Total N and phosphate uptake, determined by mass-balance, were similar across treatments averaging 67.8 μM per day and 5.4 μM per day, respectively (Fig. S3), however, instant NO_3^- uptake rates normalized to cell number indicated that HCO_2 NO_3^- cultures assimilated more NO_3^- than LCO_2 NO_3^- cultures (Fig. 1a). Under both CO_2 treatments, most of the N was assimilated during the light phase with only 14.3% NH_4^+ and 9.8% NO_3^- assimilated during the night for $NH_4^+ + NO_3^-$ and NO_3^- cultures, respectively (Fig. 1). The presence of NH_4^+ almost completely inhibited NO_3^- assimilation, with only 3.6% of the daily N

Table 2 Effect of CO_2 levels and N source in *Emiliania huxleyi* cultures

Treatment	LCO_2 $NH_4^+ + NO_3^-$	LCO_2 NO_3^-	HCO_2 $NH_4^+ + NO_3^-$	HCO_2 NO_3^-
Growth rate (day^{-1})	1.26 (a) ± 0.03	0.93 (b) ± 0.02	1.21 (a) ± 0.02	1.18 (a) ± 0.02
Days in culture	160	160	155	155
Generations	291	214	270	264
Cell volume (μm^3)	67.0 (a) ± 1.6	54.5 (b) ± 1.7	55.8 (b) ± 1.8	66.3 (a) ± 1.1
POC (fg C μm^{-3})	250.7 (a,b) ± 15	208.7 (a,b) ± 3.6	227.1 (a) ± 8.7	213.0 (b) ± 5.9
PIC (fg C μm^{-3})	104.0 (a,b) ± 3.6	171.3 (c) ± 6.3	92.9 (a) ± 4.3	135.3 (b) ± 5.0
PON (fg N μm^{-3})	30.7 (a) ± 1.7	26.6 (a) ± 0.6	28.7 (a) ± 1.1	26.4 (a) ± 0.7
PIC/POC	0.42 (a) ± 0.02	0.82 (b) ± 0.02	0.41 (a) ± 0.01	0.64 (c) ± 0.02
POC/PON	9.50 (a) ± 0.1	9.15 (a) ± 0.2	9.26 (a) ± 0.4	9.4 (a) ± 0.1
TPC/PON	13.5 (a,c) ± 0.2	16.6 (b) ± 0.3	13.0 (a) ± 0.6	15.4 (b,c) ± 0.1

Data are shown for the four cultures in each growing conditions. Low CO_2 (LCO_2) and high CO_2 (HCO_2) with $NH_4^+ + NO_3^-$ or NO_3^- as N source. Samples were taken 14 h into the light period. Except for days in culture and generations, data are given as means ± SE for at least four replicates taken every third day for each culture condition. Letters in parentheses indicate significant differences ($P < 0.01$) among treatment types using analysis of variance (ANOVA), Tukey's *post hoc* test. POC, particulate organic carbon; PIC, particulate inorganic carbon; PON, particulate organic nitrogen; TPC, total particulate carbon. Ratios are given as molar ratio.

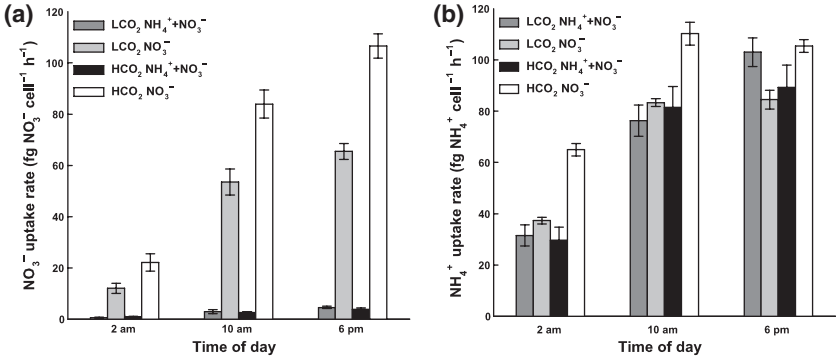

Fig. 1 Nitrogen assimilation rates of *Emiliania huxleyi* cultures. NO_3^- (a) and NH_4^+ (b) assimilation rates were determined using $K^{15}NO_3$ and $^{15}NH_4Cl$ stable isotope tracers, respectively. Measurements were made 4 and 12 h into the light phase (10 am and 6 pm, respectively) and 4 h into the dark phase (2 am) for each growth condition. LCO_2 $NH_4^+ + NO_3^-$ (dark gray bars), LCO_2 NO_3^- (light gray bars), HCO_2 $NH_4^+ + NO_3^-$ (black bars), HCO_2 NO_3^- (white bars). Data are mean ± SE of three samples taken every third day for each culture condition.

uptake sustained by NO_3^- for $NH_4^+ + NO_3^-$ cultures (Fig. 1a), while NO_3^- did not prevent NH_4^+ assimilation at both CO_2 levels (Fig. 1b).

Scanning electron microscopy images revealed incomplete and hollow coccoliths for $NH_4^+ + NO_3^-$ cultures compared to NO_3^- cultures. In contrast, differences in the pCO_2 levels had no obvious effect on coccolith morphology (Fig. 2 and Fig. S4).

^{14}C assimilation rates showed that calcification was only observed during the light phase, with rates increasing as the light period progressed (Fig. 3). At 10 am (4 h into the light phase), $NH_4^+ + NO_3^-$ cultures had lower calcification rates than NO_3^- cultures by 1.6- and 2.1-fold ($P < 0.01$), in LCO_2 and HCO_2, respectively (Fig. 3). This trend was also apparent at 6 pm (12 h into the light phase), where $NH_4^+ + NO_3^-$ cultures calcified at 1.2 and 1.9 times slower rates than NO_3^- cultures, under LCO_2 and HCO_2, respectively. Changes in calcification rates were not significant at LCO_2, but were significant ($P < 0.01$) under HCO_2 (Fig. 3).

PIC contents per cell volume at the end of the photoperiod (2 h before dark phase) were lower in $NH_4^+ + NO_3^-$ cultures compared to NO_3^- cultures by 1.6 and 1.5-fold ($P < 0.01$) in LCO_2 and HCO_2, respectively (Table 2). PIC content per cell volume also decreased under HCO_2, but the effect was smaller (1.1 and 1.3-fold compared to LCO_2, in $NH_4^+ + NO_3^-$ and NO_3^- cultures, respectively; these changes were not significant for $NH_4^+ + NO_3^-$ cultures, but significant ($P < 0.01$) for NO_3^- cultures; Table 2). No effect of CO_2

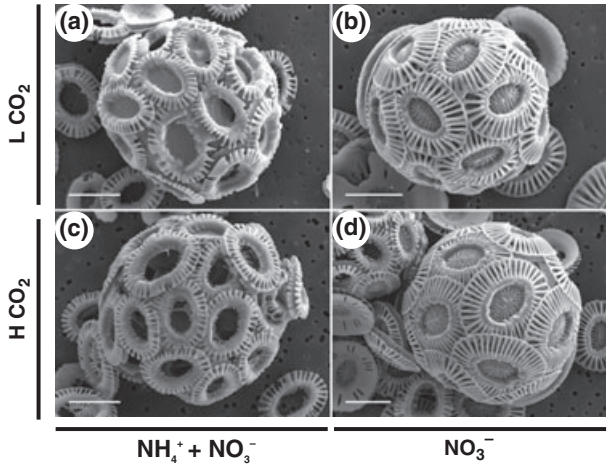

Fig. 2 Effects of N source and pCO_2 levels on coccolithophore morphology. Scanning electron microscope (SEM) images of *Emiliania huxleyi* sampled 14 h into the light period. Cultures were grown at LCO_2 with NH_4^++NO_3^- (a) or NO_3^- (b) as N source, and HCO_2 with NH_4^++NO_3^- (c) or NO_3^- (d) as N source. Scale bar 2 μm.

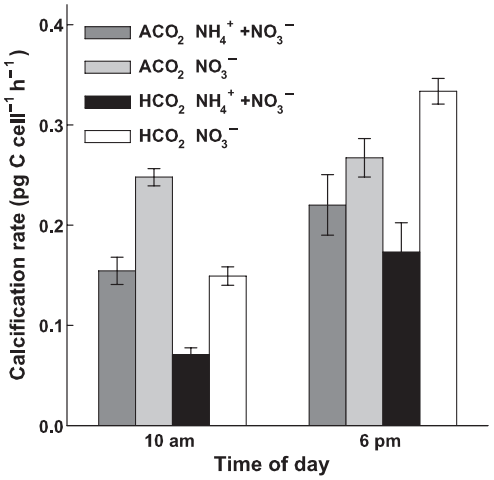

Fig. 3 Calcification rates of *Emiliania huxleyi* cultures. Measurements were determined using radio-labeled $H^{14}CO_3^-$, 4 and 12 h into the photoperiod (10 am and 6 pm, respectively) for each growth condition. LCO_2 NH_4^+ + NO_3^- (dark gray bars), LCO_2 NO_3^- (light gray bars), HCO_2 NH_4^+ + NO_3^- (black bars), HCO_2 NO_3^- (white bars). Data are mean ± SE of three samples taken every third day for each culture condition.

was observed on the POC content per cell volume for both NH_4^+ + NO_3^- and NO_3^- cultures. The presence of NH_4^+, however, increased POC content per cell volume by 20% and 7% for LCO_2 and HCO_2 cultures, respectively. The effect of NH_4^+ on POC content per cell volume was not significant in LCO_2, but was significant ($P < 0.01$) in HCO_2 (Table 2). As a result, PIC/POC

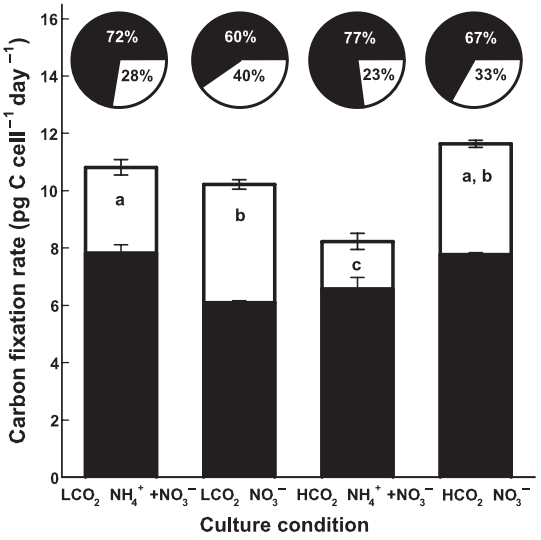

Fig. 4 Daily carbon fixation and allocation of *Emiliania huxleyi* cultures. Daily calcification rates (white) and primary production (black) were determined by integrating the measurements at 4 and 12 h into the photoperiod (10 am and 6 pm, respectively, from Fig. S5) across the light period for each growth condition: LCO_2 NH_4^+ + NO_3^-, LCO_2 NO_3^-, HCO_2 NH_4^+ + NO_3^- and HCO_2 NO_3^-. Data are mean ± SE of three samples taken every third day for each culture condition. Letters indicate significant differences ($P < 0.01$) for calcification rates among treatment types using analysis of variance (ANOVA), Tukey's *post hoc* test. Pie chart values are given as percentages.

ratios were lower by a factor of 2.0 and 1.6 ($P < 0.01$) in NH_4^+ + NO_3^- cultures compared to NO_3^- cultures, at LCO_2 and HCO_2, respectively (Table 2). Finally, PON content per cell volume and POC/PON ratios were similar across all four treatments averaging 28 fg N μm^{-3} and 9.3, respectively (Table 2). We observed a significant interaction between pCO_2 and N source on PIC content per cell volume and the PIC/POC ratio, indicating that pCO_2 and N source have a synergistic effect on *E. huxleyi* carbon partitioning (Table S2).

E. huxleyi growth rates were similar under all conditions, ranging between 1.18 and 1.26 day^{-1}, except for LCO_2 NO_3^- cells, which grew significantly slower ($P < 0.01$) by 30% (Table 2). To investigate carbon allocation, we integrated total carbon fixation per cell across the day (from Fig. S5). Primary production for LCO_2 NO_3^- cultures was the lowest of the four conditions, accounting for 60% of the total daily fixed carbon compared to 67–77% in the other three growth conditions (Fig. 4). It is also evident that calcification is a greater carbon sink in the NO_3^- cultures, representing 40% and 33% of the daily fixed carbon under LCO_2 and HCO_2, respectively, compared to NH_4^+ + NO_3^- cultures where calcification contributed 28% and 23% of

the daily fixed carbon at LCO_2 and HCO_2, respectively (Fig. 4). Growth rates were positively correlated with primary production ($R^2 = 0.57$) and negatively correlated with calcification ($R^2 = 0.42$) across all treatments (Fig. 5, Fig. S6).

We observed diel variation in cell volume that increased throughout the light phase and decreased during the night (Fig. S7). At the end of the photoperiod, under LCO_2, cells were 23% larger in $NH_4^+ + NO_3^-$ ($P < 0.01$) than in NO_3^- (Table 2, Fig. S7). The opposite pattern was observed under HCO_2, where cells were 16% smaller in $NH_4^+ + NO_3^-$ ($P < 0.01$) than in NO_3^- (Table 2 and Fig. S7). HCO_2 caused a cell size decrease by 17% ($P < 0.01$) and a cell size increase by 22% ($P < 0.01$) compared to LCO_2 for $NH_4^+ + NO_3^-$ and NO_3^- cultures, respectively (Table 2, Fig. S7).

Discussion

Recently, Barcelos e Ramos *et al.* (2010) reported that only 26 h are required to assure coccolithophore acclimation to their environment. After more than 200 generations, it is clear that our cultures were acclimated to the growing conditions. A generalization for multi-generational experiments is that after 1000 generations enough genetic variability has occurred so that the culture can be considered as a new population (Collins *et al.*, 2006). Although our experiment was conducted for 1/5 of the generations cited above, it is possible that our cultures had evolved toward adaptation to their environment (Collins, 2010; Müller *et al.*, 2010).

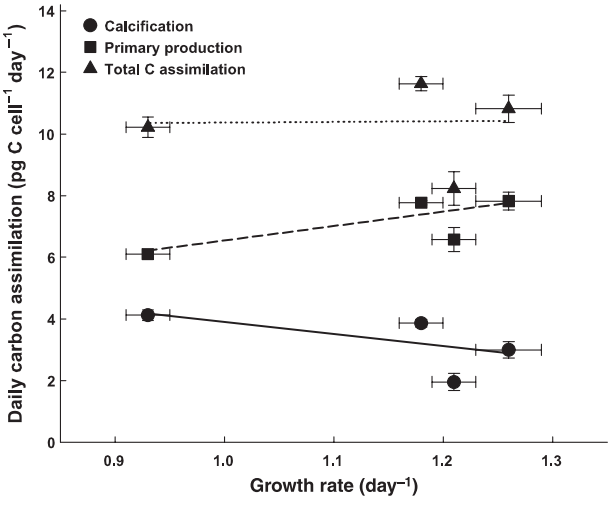

Fig. 5 Correlation between growth rates and carbon fixation. Growth rates and daily carbon fixation rates for the four treatments were derived from Table 2 and Fig. 4. Calcification rates (circles), primary production (squares) and total carbon assimilation (triangles). Corresponding linear regression equations and R^2 are: $y = -4.3x + 8.15$, $R^2 = 0.42$; $y = 4.4x + 2$, $R^2 = 0.57$ and $y = -0.16x + 10.4$, $R^2 = 0.000027$, respectively.

In our culturing conditions, excess nutrients always remained in the growing vessels, ensuring that N and PO_4^{2-} were never limiting. Daily N uptake rates and cellular PON contents in this study are in good agreement with those previously reported for *E. huxleyi* (Varela & Harrison, 1999; Leonardos & Geider, 2005). Our slightly higher values likely reflect the higher growth rate of our cultures. Our *E. huxleyi* cultures also showed a similar deviation from the Redfield C/N ratio previously reported for that species (Leonardos & Geider, 2005). Inhibition of NO_3^- uptake by NH_4^+ is well documented for phytoplankton species (Eppley *et al.*, 1969; Harrison *et al.*, 1996) and in *E. huxleyi* it is reported that 0.2 μM NH_4^+ halves NO_3^- uptake and 2.2 μM of NH_4^+ completely inhibits NO_3^- uptake (Varela & Harrison, 1999). Our study is in good agreement with these previous reports and it is possible that the 3.6% NO_3^--supported N assimilation, reported here, when both N sources were supplied was within analytical error. Only small proportions of NO_3^- and NH_4^+ were assimilated during the dark phase while the main part of N assimilation took place during the light phase, when energy and reducing power necessary for NO_3^- and NH_4^+ incorporation, are in high supply via photosynthesis.

A recent study reported increases in both calcification rate and primary production when *E. huxleyi* (strain NZEH) was grown under elevated pCO_2 (Iglesias-Rodriguez *et al.*, 2008a). Conversely, an earlier study on the same species came to a fundamentally opposite conclusion demonstrating reduced calcification in *E. huxleyi* (strain PML B92/11) exposed to elevated pCO_2 (Riebesell *et al.*, 2000). Despite the active debate that ensued (Iglesias-Rodriguez *et al.*, 2008b; Riebesell *et al.*, 2008), the cause for this discrepancy is still unclear. Divergent physiologic responses to ocean acidification have also been proposed to be due to genetic differences among strains of *E. huxleyi* (Langer *et al.*, 2009; Beaufort *et al.*, 2011). In our study, night calcification was negligible and significant rates of calcification were only observed during the light phase, with calcification rate increasing as the light period progressed, reinforcing previously shown coupling of photosynthetic end-products production with calcification intensity (Paasche, 1964, 1966, 2002). We observed a reduction in calcification rate and cellular PIC content at elevated pCO_2. These results are consistent with another study using the same *E. huxleyi* strain (CCMP 371) that demonstrated reduction in the cellular PIC with increasing pCO_2 levels or with increasing light intensity (Feng *et al.*, 2008).

More interestingly, we observed that the N source had a stronger effect on calcification than pCO_2. Our study demonstrates that calcification was enhanced under NO_3^- assimilation and reduced under NH_4^+ assimilation. Given that NO_3^- assimilation requires more reducing power relative to NH_4^+ assimilation, it is possible that the observed effect on calcification is linked to a change in the redox status of the cell, which might be exacerbated under low CO_2 when the primary carbon reduction (Calvin–Benson) cycle is a more restricted sink for reducing power. Another possible explanation would involve the excess protons generated during NH_4^+ assimilation. The assimilation of 3 moles of N as NO_3^- produces 2 moles of excess OH^- ions, whereas assimilation of 3 moles of N as NH_4^+ produces 4 moles of excess H^+ (Raven, 1986). To maintain intracellular pH homeostasis, excess H^+ needs to be moved out of the cell across the cell membrane. The H^+ movement could be facilitated by the high membrane permeability for H^+ recently demonstrated in *E. huxleyi* (Suffrian *et al*., 2011; Taylor *et al*., 2011). Nevertheless, it is possible that the excess H^+ generated by NH_4^+ assimilation would reduce the internal conversion of HCO_3^- to CO_3^{2-} and H^+, thereby restricting the availability of CO_3^{2-} for $CaCO_3$ production. Conversely, the OH^- generated during NO_3^- assimilation could combine with the H^+ generated during HCO_3^- dissociation to CO_3^{2-}, thus promoting calcification.

Previous studies have indicated that *E. huxleyi* possesses only NADH specific NO_3^- reductase, a characteristic shared with the red algae lineage in comparison with the NAD(P)H bi-specific NO_3^- reductases of green algae and higher plants (Iwamoto & Shiraiwa, 2003). The K_m of NO_3^- reductase in *E. huxleyi* for NADH was found to be high (23–80 μM), similar to the one found in red algae, in comparison with the lower K_m for NADH (3–5 μM) found in higher plants and diatoms (Iwamoto & Shiraiwa, 2003). The apparent poor NO_3^- reductase affinity for its substrates in *E. huxleyi* was proposed to be compensated by high NO_3^- transporter affinities (Iwamoto & Shiraiwa, 2003). Although this can not be excluded, searches of *E. huxleyi* CCMP 1516's genome indicate 24 predicted NH_4^+ transporter genes (12 supported by EST), but only eight predicted NO_3^- transporter genes, supporting previous studies (Muggli & Harrison, 1996) suggesting that these cells may be more greatly poised to transport NH_4^+ than NO_3^- in comparison with other phytoplankton species.

Under low CO_2, for the same amount of N consumed by the cells, the faster growth rate supported by NH_4^+ assimilation may be due to the lower reducing power required for NH_4^+ assimilation in comparison to NO_3^- assimilation. This advantage is offset by increased CO_2 availability, possibly because the cells do not need to invest as many resources for carbon acquisition and assimilation (e.g., carbon concentration mechanisms). Although the relationship slopes were quite small, the cultures growth rates were positively correlated to primary production, but negatively correlated to calcification, that is, the more the cells calcify the less primary production they can achieve and the slower they grow. Although speculative, it has been proposed that the coccolithophore $CaCO_3$ exoskeleton might confer a protective advantage (Young, 1994; Irie *et al*., 2010) and the relation above might reflect a balance between protection and growth speed.

This study demonstrates that N source and pCO_2 synergistically impact cell volume. It is important to note that cell sizes were determined including the coccolith layers, but since NO_3^- cells calcified more than $NH_4^+ + NO_3^-$ cells, the larger cell size observed for $NH_4^+ + NO_3^-$ cells under LCO_2 was unlikely to be due to a thicker coccolith layer, but rather resulted from an effect of N source. These results emphasize the need to assess various environmental parameters in combination, to develop accurate predictions of phytoplankton responses to ocean acidification. A recent study indicated that elevated pCO_2 reduces iron bioavailability, thus increasing iron stress for phytoplankton (Shi *et al*., 2010). Feng *et al.* (2009) also reported change in community structure in a North Atlantic spring bloom with increased organic carbon fixation rate and weakened calcification in response to elevated pCO_2 and temperature. More studies assessing the synergistic effect of various factors such as, pCO_2 levels and phosphate availability will be needed in the future to complement our current knowledge (Leonardos & Geider, 2005; De Bodt *et al*., 2010; Gao & Zheng, 2010) and help building our understanding of the full extent of direct and indirect consequences of ocean acidification on phytoplankton.

In a recent report, Beman *et al.* (2011) estimated that at least 1% and up to 25% of global marine primary production would be supported by regenerated NH_4^+ rather than NO_3^- in the future acidified ocean. Assuming that CO_2/N source-related responses of the coccolithophore *E. huxleyi* as described in this study (6% reduction in calcification due to elevated pCO_2 alone and 53% reduction for combined elevated pCO_2 and NH_4^+-supported regenerated production) are representative for overall *E. huxleyi* species biogenic calcification, and using the estimates of NH_4^+ supported primary production cited above, the potential impact of combined elevated CO_2 and shifts from NO_3^--supported new production to NH_4^+-supported regenerated production can be estimated to reduce calcification by 7–18% per year compared to a reduction of 6% per year resulting from elevated CO_2 alone.

The overall effect of ocean acidification, rising sea surface temperatures and anthropogenic N emissions is predicted to increase the oceanic NH_4^+/NO_3^- ratio, and that under such conditions, *E. huxleyi* has been proposed to dominate phytoplankton communities (Eppley *et al*., 1969; Feng *et al*., 2009). If the findings presented above are also applicable to cells grown under nutrient-limiting conditions, our study would suggest that compared to increasing CO_2 alone, a greater reduction of coccolithophores calcification, thus a greater disruption of the organic carbon pump, could be expected in response to the combined effect of increased NH_4^+/NO_3^- ratio and CO_2 level in the future acidified ocean. In this study, experiments were conducted with a single species and to generate the sufficient biomass necessary for the determination of the different parameters, the nutrient concentrations were maintained at much higher levels than usually found in the open ocean. Thus, to extend our findings to the global carbon cycle our results should be further assessed with other coccolithophore species and under lower and more realistic oceanic nutrient concentrations.

Acknowledgements

We are thankful to Drs BA Read and RJ Geider for helpful comments and insight in the writing of this manuscript, Dr RC Dugdale for guidance and assistance with ^{15}N analysis, and Dr AS Ichimura for assistance with SEM imaging. This work was supported by NSF BIO-OCE 0723908 to EJC, JHS and TK; NSF-MRI awards 0727179 to TK. SEM was funded by NSF-MRI award 0821619 to ASI.

References

Armstrong RA, Lee C, Hedges JI, Honjo S, Wakeham SG (2002) A new mechanistic model for organic carbon fluxes in the ocean: based on the quantitative association of POC with ballast minerals. *Deep Sea Research*, **49**, 219–236.

Balch WM, Holligan PM, Kilpatrick KA (1992) Calcification, photosynthesis and growth of the bloom-forming coccolithophore, *Emiliania huxleyi*. *Continental Shelf Research*, **12**, 1353–1374.

Barcelos e Ramos J, Biswas H, Schultz KG, LaRoche J, Riebesell U (2007) Effect of rising atmospheric carbon dioxide on the marine nitrogen fixer Trichodesmium. *Global Biogeochemical Cycles*, **21**, GB2028.1–GB2028.6.

Barcelos e Ramos J, Müller MN, Riebesell U (2010) Short-term response of the coccolithophore *Emiliania huxleyi* to an abrupt change in seawater carbon dioxide concentrations. *Biogeosciences*, **7**, 177–186.

Beaufort L, Probert I, de Garidel-Thoron T *et al*. (2011) Sensitivity of coccolithophores to carbonate chemistry and ocean acidification. *Nature*, **476**, 80–83.

Beman JM, Chow C-E, King AL *et al*. (2011) Global declines in oceanic nitrification rates as consequence of ocean acidification. *Proceedings of the National Academy of Sciences*, **108**, 208–213.

Bradshaw AL, Brewer PG, Shaffer DK, Williams RT (1981) Measurements of total carbon dioxide and alkalinity by potentiometric titration in the GEOSECS program. *Earth and Planetary Science Letters*, **55**, 99–115.

Collins S (2010) Comment on Effects of long-term high CO_2 exposure on two species of coccolithophores. *Biogeosciences*, **7**, 2199–2202.

Collins S, Sültemeyer D, Bell G (2006) Changes in C uptake in populations of *Chlamydomonas reinhardtii* selected at high CO_2. *Plant, Cell and Environment*, **29**, 1812–1819.

De Bodt C, Van Oostende N, Harlay J, Sabbe K, Chou L (2010) Individual and interacting effects of pCO_2 and temperature on *Emiliania huxleyi* calcification: study of the calcite production, the coccolith morphology and the coccosphere size. *Biogeosciences*, **7**, 1401–1412.

Dickson AG, Millero FJ (1987) A comparison of the equilibrium constants for the dissociation of carbon acid in seawater media. *Deep-Sea Research*, **34**, 1733–1743.

Dugdale RC (1967) Nutrient limitation in the sea: dynamics, identification, and significance. *Limnology and Oceanography*, **12**, 685–695.

Dugdale RC, Wilkerson FP (1986) The use of ^{15}N to measure nitrogen uptake in eutrophic oceans; experimental considerations. *Limnology and Oceanography*, **31**, 673–680.

Eppley RW, Rogers JN, McCarthy JJ (1969) Half-saturation constants for uptake of nitrate and ammonium by marine phytoplankton. *Limnology and Oceanography*, **14**, 912–920.

Feng Y, Warner ME, Zhang Y, Sun J, Fu FX, Rose JM, Hutchins DA (2008) Interactive effects of increased pCO_2, temperature, and irradiance on the marine coccolithophore *Emiliania huxleyi* (Prymnesiophyceae). *European Journal of Phycology*, **43**, 87–98.

Feng Y, Clinton EH, LeBlanc K *et al*. (2009) Effects of increased pCO_2 and temperature on the North Atlantic spring bloom. I. The phytoplankton community and biogeochemical response. *Marine Ecology-Progress Series*, **388**, 13–25.

Francois R, Honjo S, Krishfield R, Manganini S (2002) Factors controlling the flux of organic carbon to the bathypelagic zone of the ocean. *Global Biogeochemical Cycles*, **16**, 1087, doi: 10.1029/2001GB001722.

Friederich GE, Walz PM, Burczynski MG, Chavez FP (2002) Inorganic carbon in the central California upwelling system during the 1997-1999 El Nino – La Nina event. *Progress in Oceanography*, **54**, 185–203.

Gao K, Zheng Y (2010) Combined effects of ocean acidification and solar UV radiation on photosynthesis, growth, pigmentation and calcification of the coralline alga *Corallina sessilis* (Rhodophyta). *Global Change Biology*, **16**, 2388–2398.

Gran G (1952) Determination of the equivalence point in potentiometric titrations of seawater with hydrochloric acid. *Oceanologica Acta*, **5**, 209–218.

Guillard RRL, Ryther JH (1962) Studies of marine plankton diatoms. I. Cyclotella nana Hustedt and Detonula confervacea (Cleve). *Canadian Journal of Microbiology*, **8**, 229–239.

Harrison WG, Harns LR, Irwin BD (1996) The kinetics of nitrogen utilization in the oceanic mixed layer: nitrate and ammonium interactions at nanomolar concentrations. *Limnology and Oceanography*, **41**, 16–32.

Holmes RM, Aminot AK, Hooker BA, Peterson BJ (1999) A simple and precise method for measuring ammonium in marine and freshwater ecosystems. *Canadian Journal of Fisheries and Aquatic Sciencies*, **56**, 1801–1808.

Huesemann MH, Skillman AD, Crecelius EA (2002) The inhibition of marine nitrification by ocean disposal of carbon dioxide. *Marine Pollution Bulletin*, **44**, 142–144.

Hutchins DA, Fu FX, Zhang Y, Warner ME, Portune K, Bernhardt PW, Mulholland MR (2007) CO_2 control of Trichodesmium photosynthesis, growth rates, and elemental ratios: implications for past, present and future ocean biochemistry. *Limnology and Oceanography*, **52**, 1293–1304.

Hutchins DA, Mulholland MR, Fu FX (2009) Nutrient cycles and marine microbes in a CO_2-enriched ocean. *Oceanograhy*, **22**, 128–145.

Iglesias-Rodriguez MD, Halloran PR, Rickaby RE *et al*. (2008a) Phytoplankton calcification in a high-CO_2 world. *Science*, **320**, 336–340.

Iglesias-Rodriguez MD, Buitenhuis ET, Raven JA *et al*. (2008b) Response to comment on Phytoplankton calcification in a high-CO_2 world. *Science*, **322**, 1466.

Irie T, Bessho K, Findlay HS, Calosi P (2010) Increasing costs due to ocean acidification drives phytoplankton to be more heavily calcified: optimal growth strategy of coccolithophores. *PLoS ONE*, **5**, 13436, doi: 10.1371/journal.pone.0013436.

Iwamoto K, Shiraiwa Y (2003) Characterization of NADH: nitrate reductase from the coccolithophorid *Emiliania huxleyi* (Lohman) Hay and Mohler (Haptophyceae). *Marine Biotechnology*, **5**, 20–26.

Klaas C, Archer DE (2002) association of sinking organic matter with various types of mineral ballast in the deep sea: implication for the rain ratio. *Global Biogeochemical Cycles*, **16**, 1116, doi: 10.1029/2001GB001765.

Kranz S, Sültemeyer D, Richter KU, Rost B (2009) Carbon acquisition by Trichodesmium: the effect of pCO_2 and diurnal changes. *Limnology and Oceanography*, **54**, 548–559.

Kroeker KJ, Kordas RL, Crim RN, Singh GG (2010) Meta-analysis reveals negative yet variable effects of ocean acidification on marine organisms. *Ecology Letters*, **11**, 1304–1315.

Langer G, Nehrke G, Probert I, Ly J, Ziveri P (2009) Strain-specific responses of *Emiliania huxleyi* to changing seawater carbonate chemistry. *Biogeosciences*, **6**, 2637–2646.

Lefebvre SC, Harris G, Webster R *et al*. (2010) Characterisation and expression analysis of the *Lhcf* gene family in *Emiliania huxleyi* (Haptophyta) reveals differential responses to light and CO_2. *Journal of Phycology*, **46**, 123–134.

Leonardos N, Geider RJ (2005) Elevated atmospheric carbon dioxide increases organic carbon fixation by *Emiliania huxleyi* (Haptophyta), under nutrient-limited high-light conditions. *Journal of Phycology*, **41**, 1196–1203.

Levitan O, Rosenberg G, Setlik I, Setlikova E, Grigel J, Klepetar J (2007) Elevated CO_2 enhances nitrogen fixation and growth in the marine cyanobacterium Trichodesmium. *Global Change Biology*, **13**, 531–538.

Lewis E, Wallace DWR (1998) *Program Developed for CO2 System Calculations ORNL/CDIAC-105*. Carbon Dioxide Information Analysis Center, Oak Ridge National Laboratory, US Department of Energy, Oak Ridge, TN.

Mehrbach C, Culberson CH, Hawley JE, Pytkovicz RM (1973) Measurement of the apparent dissociation constants of carbonic acid in seawater at atmospheric pressure. *Limnology and Oceanography*, **18**, 897–907.

Muggli DL, Harrison PJ (1996) Effects of nitrogen source on the physiology and metal nutrition of *Emiliania huxleyi* grown under different iron and light conditions. *Marine Ecology-Progress Series*, **130**, 255–267.

Mulholland MR, Lomas M (2008) Nitrogen uptake and assimilation. In: *Nitrogen in the Marine Environment* (eds Capone DG, Bronk DA, Mulholland MR, Carpenter EJ), pp. 303–385. Elsivier press, Amsterdam.

Müller MN, Schulz KG, Riebesell U (2010) Effects of long-term high CO_2 exposure on two species of coccolithophores. *Biogeosciences*, **7**, 1109–1116.

Nanninga HJ, Tyrrell T (1996) Importance of light for the formation of algal bloom by *Emiliania huxleyi*. *Marine Ecology-Progress Series*, **136**, 195–203.

Paasche E (1964) A tracer study of the inorganic carbon uptake during coccolith formation and photosynthesis in coccolithophorid *Coccolithus huxleyi*. *Physiologia Plantarum*, **3**, 78–82.

Paasche E (1966) Adjustment to light and dark rates of coccolith formation. *Physiologia Plantarum*, **19**, 271–278.

Paasche E (2002) A review of the coccolithophorid *Emiliania huxleyi* (Prymnesiophyceae), with particular reference to growth, coccolith formation, and calcification-photosynthesis interactions. *Phycologia*, **40**, 503–529.

Raven JA (1986) Biochemical disposal of excess H^+ in growing plants? *New Phytologist*, **104**, 175–206.

Riebesell U, Zondervan I, Rost B, Tortell PD, Zeebe RE, Morel FMM (2000) Reduced calcification of marine plankton in response to increased atmospheric CO_2. *Nature*, **407**, 364–367.

Riebesell U, Bellerby RGJ, Engel A *et al*. (2008) Comment on Phytoplankton calcification in a high-CO_2 world. *Science*, **322**, 1466.

Rost B, Riebesell U (2004) Coccolithophore calcification and the biological pump: response to environmental changes. In: *Coccolithophores, from Molecular Processes to Global Impact* (eds Thierstein HR, Young JR), pp. 99–125. Springer, Berlin.

Ryther JH, Dunstan WM (1971) Nitrogen, phosphorus, and eutrophication in the coastal marine environment. *Science*, **171**, 1008–1013.

Samiento JL, Hughes TMC, Stouffer RJ, Manabe S (1998) Simulated response of the ocean carbon cycle to anthropogenic climate warming. *Nature*, **393**, 245–249.

Sciandra A, Harlay J, Lefèvre D, Lemée R, Rimmelin P, Denis M, Gattuso J-P (2003) Response of coccolithophorid *Emiliania huxleyi* to elevated partial pressure of CO_2 under nitrogen limitation. *Marine Ecology-Progress Series*, **261**, 111–122.

Sharp JH (1983) The distribution of inorganic nitrogen and dissolved and particulate organic nitrogen in the sea. In: *Nitrogen in the Marine Environment* (eds Carpenter EJ, Capone DG), pp. 1–35. Academic Press, New York.

Sharp JH, Yoshiyama K, Parker AE *et al*. (2009) The chemistry of the Delaware Estuary: seasonal and spatial trends and correlations. *Estuaries and Coasts*, **32**, 1023–1043.

Shi D, Xu Y, Hopkinson BM, Morel FM (2010) Effect of ocean acidification on iron availability to marine phytoplankton. *Science*, **327**, 676–679.

Solorzano L (1969) A method for measuring ammonium in seawater. *Limnology and Oceanography*, **14**, 799–801.

Suffrian K, Schulz KG, Gutowska MA, Riebesell U, Bleich M (2011) Cellular pH measurements in *Emiliania huxleyi* reveal pronounced membrane proton permeability. *New Phytologist*, **190**, 595–608.

Taylor AR, Chrachri A, Wheeler G, Goddard H, Brownlee C (2011) A voltage-gated H^+ channel underlying pH homeostasis in calcifying coccolithophores. *PLOS Biology*, **9**, 1–14.

Thierstein HR, Geitzenauer KR, Molfino B (1977) Global synchroneity of late quaternary coccolith datum levels-validation by oxygen isotopes. *Geology*, **5**, 400–404.

Varela DE, Harrison PJ (1999) Effect of ammonium on nitrate utilization by *Emiliania huxleyi*, a coccolithophore from the oceanic northeastern Pacific. *Marine Ecology-Progress Series*, **186**, 67–74.

de Vargas C, Aubry MP, Probert I, Young J, Falkowski P, Knoll AH (2007) Origin and evolution of coccolithophores: from coastal hunters to oceanic farmers. In: *Evolution of Aquatic Photoautotrophs* (eds Falkowski P, Knoll AH), pp. 251–281. Elsevier Academic, New York.

Ward BB (1987) Kinetic studies on ammonia and methane oxidation by *Nitrosococcus oceanus*. *Archives of Microbiology*, **147**, 126–133.

Whitledge TE, Malloy SC, Patton CJ, Wirick CD (1981) *Automated Nutrient Analyses in Seawater*. Brookhaven National Laboratory, Upton, NY, BLN 51398.

Wyatt NJ, Kitidis V, Woodward EMS, Rees AP, Widdicombe S (2010) Effects of high CO_2 on the fixed nitrogen inventory of the Western English Channel. *Journal of Plankton Research*, **0**, 1–11.

Young JR (1994) Functions of coccoliths. In: *Coccolithophores* (eds Winter A, Siesser WG), pp. 63–82. Cambridge University Press, Cambridge.

Zondervan I, Zeebe RE, Rost B, Riebesell U (2001) Decreasing marine biogenic calcification: a negative feedback on rising atmospheric pCO_2. *Global Biogeochemical Cycles*, **15**, 507–516.

Supporting Information

Additional Supporting Information may be found in the online version of this article:

Figure S1. Steady-state concentrations of nutrients in cultures and total nitrogen and phosphorous consumed. Nutrients were measured in the four reactors with steady-state densities of *Emiliania huxleyi* at 500 000 cell mL^{-1}. Nitrogen (N) and phosphate consumed were derived as the difference between the steady-state concentrations in the cyclostats and that in the inflow-media. Low CO_2 and $NH_4^+ + NO_3^-$ (LCO_2 $NH_4^+ + NO_3^-$, dark gray bars), low CO_2 and NO_3^- (LCO_2 NO_3^-, light gray bars), high CO_2 and $NH_4^+ + NO_3^-$ (HCO_2 NH_4^++NO_3^-, black bars) and high CO_2 and NO_3^- (HCO_2 NO_3^-, white bars). Data are mean ± SE of at least four samples taken every third day for each culture condition.
Figure S2. pH and pCO_2 diurnal variation in *Emiliania huxleyi* cultures.
Figure S3. Growth curves of *Emiliania huxleyi* cultures on different NH_4^+ concentrations.
Figure S4. Effects of N source and pCO_2 levels on coccolithophore morphology. Scanning electron microscope (SEM) images of *Emiliania huxleyi* sampled 14 h into the light period. Cultures were grown at low CO_2 with $NH_4^+ + NO_3^-$ (a) or NO_3^- (b) as N source, and high CO_2 with $NH_4^+ + NO_3^-$ (c) or NO_3^- (d) as N source. Scale bar in overview images 10 μm, scale bar in detail images 2 μm.
Figure S5. Instant calcification rates and primary production rates of *Emiliania huxleyi* cultures. Measurements were determined using radio-labeled $H^{14}CO_3$, 4 and 12 hours into the photoperiod (10 am and 6 pm, a and b respectively) for each growth condition. Low CO_2 with $NH_4^+ + NO_3^-$ (LCO_2 $NH_4^+ + NO_3^-$), low CO_2 with NO_3^- (LCO_2 NO_3^-), high CO_2 with $NH_4^+ + NO_3^-$ (HCO_2 $NH_4^+ + NO_3^-$), high CO_2 and NO_3^- (HCO_2 NO_3^-). Bar chart data are given as mean ± SE for at least three replicates taken every third day for each culture condition. Pie charts are given as percentages.
Figure S6. Correlation between growth rates and particulate carbon content. PIC, POC and TPC were determined at 14 h into the light phase (2 h before the dark phase). PIC (blue circles), POC (red squares) and TPC (green triangles). Corresponding linear regression equations and R^2 are: $y = -5.2x + 13.6$, $R^2 = 0.25$; $y = 11.1x + 1$, $R^2 = 0.76$ and $y = 5.89x + 14.6$, $R^2 = 0.1625$, respectively.
Figure S7. *Emiliania huxleyi* cell volume for each growth condition. Cell volumes were determined by flow cytometry, four hours after the dark onset (2 am) and four, eight, 12 and 14 h after the light onset (10 am, 2 pm, 6 pm, 8 pm, respectively) for each growth condition. LCO_2 $NH_4^+ + NO_3^-$ (dark gray bars), LCO_2 NO_3^- (light gray bars), HCO_2 $NH_4^+ + NO_3^-$ (black bars), HCO_2 NO_3^- (white bars). Data are mean ± SE, the number of samples (*n*, taken every third day for each culture condition) is 6, 2, 7, 2, 6 at 2 am, 10 am, 2 pm, 6 pm and 8 pm, respectively.
Table S1. Growth rates and maximum PSII photosynthetic efficiencies of *Emiliania huxleyi* cultures on different NH_4^+ concentrations.
Table S2. pCO_2 and N source interaction.

Please note: Wiley-Blackwell are not responsible for the content or functionality of any supporting materials supplied by the authors. Any queries (other than missing material) should be directed to the corresponding author for the article.